OFFICE OF NAVAL RESEARCH

Grant or Contract N00014-91WX-24155

R&T Code 4134053

Technical Report No. 9

Percolation Effects and Oxygen Inhomogeneities in $YBa_2Cu_3O_{7-\delta}$ Crystals

by

M. S. Osofsky, J. L. Cohn, E. F. Skelton, M. M. Miller,
R. J. Soulen, Jr., and S. A. Wolf
Naval Research Laboratory
Washington, DC 20375-5000

T. A. Vanderah
Chemistry Division, Research Department
Naval Weapons Center, China Lake, CA 93555

Submitted for publication in
Phys. Rev. B

October 1991

REPORT DOCUMENTATION PAGE

Form Approved
OMB No. 0704-0188

1. AGENCY USE ONLY *(Leave blank)*	2. REPORT DATE	3. REPORT TYPE AND DATES COVERED
	Oct 91	Technical Report #9 10/90-9/91

4. TITLE AND SUBTITLE
Percolation Effects and Oxygen Inhomogeneities in $YBa_2Cu_3O_{7-\delta}$ Crystals

5. FUNDING NUMBERS
N00014-91WX-24155

6. AUTHORS
M. S. Osofsky, J. L. Cohn, E. F. Skelton, M. M. Miller, R. J. Soulen, Jr., S. A. Wolf and T. A. Vanderah

7. PERFORMING ORGANIZATION NAME(S) AND ADDRESS(ES)
Naval Weapons Center
China Lake, CA 93555-6001

8. PERFORMING ORGANIZATION REPORT NUMBER

9. SPONSORING/MONITORING AGENCY NAMES(S) AND ADDRESS(ES)
Office of Naval Research (Chemistry Program)
800 N. Quincy Street
Arlington, Va 22217

10.. SPONSORING/MONITORING AGENCY REPORT NUMBER

11. SUPPLEMENTARY NOTES
Submitted to Phys. Rev. B

12a. DISTRIBUTION /AVAILABILITY STATEMENT
Approved for public release; distribution is unlimited.

12b. DISTRIBUTION CODE

13. ABSTRACT *(Maximum 200 words)*

The magnetization curves of $YBa_2Cu_3O_{7-\delta}$ crystals are widely observed to exhibit a pronounced low field minimum in the temperature range $30K<T<T_c$. We demonstrate that these magnetization anomalies correlate with the c-axis lattice parameter, and hence with the specific oxygen deficiency, δ. We interpret this low-field feature in terms of a field-induced decoupling of regions of oxygen-rich material by boundaries of oxygen-poor material, a phenomenon reminiscent of the behavior in granular superconductors. A "phase diagram" which demarcates the multi-grain onset as a function of temperature and δ is then constructed. The shape of the "phase boundaries" is described using a percolation model. This analysis demonstrates that magnetization is a very sensitive measure of crystal quality.
PACS #'s: 74.30.Ci, 74.60.Mj, 74.70.Vy

14. SUBJECT TERMS	15. NUMBER OF PAGES
	16. PRICE CODE

17. SECURITY CLASSIFICATION OF REPORT	18. SECURITY CLASSIFICATION OF THIS PAGE	19. SECURITY CLASSIFICATION OF ABSTRACT	20. LIMITATION OF ABSTRACT
UNCLASSIFIED	**UNCLASSIFIED**	**UNCLASSIFIED**	

Revised 9/9/91

Submitted to Phys Rev B 9/91

Percolation Effects and Oxygen Inhomogeneities in $YBa_2Cu_3O_{7-\delta}$ Crystals

M.S. Osofsky, J.L. Cohn, E.F. Skelton, M. M. Miller, R.J. Soulen, Jr., and S.A. Wolf

Naval Research Laboratory

Washington, DC 20375-5000

T.A. Vanderah

Naval Weapons Center

China Lake, CA 93555-6001

The magnetization curves of $YBa_2Cu_3O_{7-\delta}$ crystals are widely observed to exhibit a pronounced low field minimum in the temperature range $30K<T<T_c$. We demonstrate that these magnetization anomalies correlate with the c-axis lattice parameter, and hence with the specific oxygen deficiency, δ. We interpret this low-field feature in terms of a field-induced decoupling of regions of oxygen-rich material by boundaries of oxygen-poor material, a phenomenon reminiscent of the behavior in granular superconductors. A "phase diagram" which demarcates the multi-grain onset as a function of temperature and δ is then constructed. The shape of the "phase boundaries" is described using a percolation model. This analysis demonstrates that magnetization is a very sensitive measure of crystal quality.

PACS #'s: 74.30.Ci, 74.60.Mj, 74.70.Vy

Introduction

Magnetization curves of single crystals of $YBa_2Cu_3O_{7-\delta}$ (YBCO) invariably exhibit anomalous features: a minimum at low magnetic fields (0-2T) as well as a high field (2-6T) maximum. Kupfer et al.[1] asserted that these crystals showed granular behavior in which intergrain J_c's were strongly field dependent. Sulpice et al.[2] studied the remnant magnetization of several crystals as a function of crystal radius and did not observe size scaling. By subdividing a crystal using laser ablation, Yeshurun et al.[3] found that the remnant magnetization of samples divided into sections smaller than several hundred micrometers did scale with size at 5K. This was not true for crystals divided into larger sections. These results were interpreted as a restriction of the current flow due to defects impeding current flow. Daeumling et al.[4] examined the size dependence of magnetization at various temperatures below T_c by subdividing individual crystals. They found that from ~30-80K the magnetization curves scaled with sample radius at low fields, but not in the high field regime, which is consistent with a granular model. The authors concluded that the likely source of the granularity was oxygen defects. At lower temperatures they saw no evidence for granular behavior. Welp et al.[5] conducted a similar study and saw evidence for scaling with size.

While these experiments suggest that sample inhomogeneities are generally present in crystals of YBCO their origin is unclear. Since the coherence length of this system is on the order of tens of Angstroms, these inhomogeneities are likely to influence magnetic

and transport properties. Distinguishing such extrinsic effects from intrinsic properties is essential for improving our understanding of superconductivity in the high T_c materials.

In this paper we present the results of a systematic study of $YBa_2Cu_3O_{7-\delta}$ crystals employing measurements of x-ray diffraction, magnetization, ac susceptibility and resistivity. Our principal finding is that there is an unmistakable correlation between the low field minimum in the magnetization (at a field H_{min}) and the c-axis lattice parameter. We relate the c-axis parameter to the oxygen deficiency parameter, δ, using the results of Parks et al.[6], and thus derive the dependencies of H_{min} on δ and T. We confirm that crystals exhibit behaviors characteristic of homogeneous superconductors for $H<H_{min}$ and inhomogeneous superconductors for $H>H_{min}$. The granular-like behavior observed for $H>H_{min}$ is due to the restriction of supercurrent flow by clusters of oxygen defects which allows excess flux to enter the crystal. The observed $H_{min}(\delta)$ data are then described by a two dimensional percolation model for oxygen defects which mitigate the supercurrents. These data demonstrate that magnetization is an especially sensitive measure of crystal homogeneity.

Sample Preparation

Crystals were grown using a self-decanting BaO:CuO flux method[7] adapted from the procedures reported by Sadowski and Scheel.[8] Starting materials were Y_2O_3, $BaCO_3$, and CuO of 99.99% or

higher purity. The composition chosen for the melt was 10.2 wt% $YBa_2Cu_3O_7$-mixture in a BaO:CuO 0.28:0.72 mol eutectic solvent (m.p. near 890°C), resulting in an overall molar charge composition of 1:18.4:45.1 = Y:Ba:Cu. This particular mixture features a relatively large concentration of solvent and was reported[8] to yield thick, multimillimeter-sized $YBa_2Cu_3O_{7-\delta}$ crystals. The components were mixed by grinding with an agate mortar and pestle for 30 minutes; reactions were carried out in zirconia crucibles in order to minimize the introduction of impurity ions into the superconducting crystals. Semiquantitative elemental analyses by electron microscopy (SEM/EDX), showed that clean crystal surfaces were impurity free, whereas trace levels of zirconium were just detectable in frozen flux droplets. In a typical crystal growth experiment, a 20-25 g charge was packed into a 10 ml round-bottom zirconia crucible and heated in a muffle furnace according to the following schedule: heat to 990°C in 3.5 h, soak 20-24h, step-cool to 950°C, cool at 0.4°C/h to 870°C, cool in 96h to room temperature. Crystals grew as projections from the crucible walls and were easily extracted mechanically. Post-growth anneals were carried out under flowing oxygen at 1 atm. In a typical annealing procedure, the crystals were first heated over several hours to 800-850°C, cooled in 24h to 700°C, soaked 96h at 700°C, cooled over 24h to the annealing temperature, soaked for various times, and then finally cooled in 24h to room temperature. Annealing temperatures ranged from 420-565°C; soak times from several days to a month (see table I). In general, the preheating step at 700-850°C seemed to produce a

greater number of samples with sharper superconducting transitions and higher onset temperatures.

The oxygen content of each crystal was estimated from its measured c-axis lattice parameter using the data reported by Parks et al.[6]; In that work, c-axis determinations from refined x-ray powder diffraction data were correlated with oxygen content obtained by *iodometric* titration. To this data set were added two additional data points for: 1) tetragonal $YBa_2Cu_3O_{6.0}$ from a single crystal x-ray diffraction structure determination (a=3.863(2), c=11.830(4)Å)[9]; and 2) a near fully oxygenated, high quality (purity and T_c) polycrystalline sample that was synthesized and chemically analyzed by bromo/iodometric titration[10] in this study (a=3.8838(8), b=3.8164(4), c=11.664(1)Å; $YBa_2Cu_3O_{6.98\pm0.01}$). A linear fit of these data yields the relation c(Å)=12.8714-0.1728x, where x=(7-δ) as it appears in $YBa_2Cu_3O_{7-\delta}$.

To determine the c-axis length, each crystal was mounted and aligned on an automated 4-circle diffractometer. The (0,0,11) and (0,0, $\bar{1}$ $\bar{1}$) diffraction peaks, excited with Cu-$K\alpha_1$ radiation, were each centered using a standard centering procedure. The $K\alpha_1$-$K\alpha_2$ doublets were then measured by step scanning in $\pm2\theta$ in 0.02° steps. These data were then least-squares fitted to double-Gaussian curves to determine centroids of all four peaks, from which c was calculated. The scatter in the values of the c-axis was typically about ±0.003%, which corresponds to an uncertainty in oxygen content of about ±0.03%. This uncertainty is much smaller than the scatter in the c-axis versus δ data of reference 6 which yields an uncertainty in δ of approximately ±0.03 to 0.04.

Magnetization

Magnetization data, M(H), were obtained at several temperatures for each crystal in a Quantum Design SQUID magnetometer. The samples were cooled in a 0±30G field and warmed above the superconductive transition temperature, T_c, between each temperature run. In all cases the field was oriented along the crystalline c-axis so that the M(H) data reflect shielding currents which flow in the a-b plane. Figures 1a and 1b show the dip at H_{min} for several temperatures for a crystal with a nominal deficiency, $\delta \sim 0.15$. At this nominal oxygen composition, H_{min} increases with decreasing temperature. Whenever possible the value for H_{min} is determined from the initial ascending field sweep to avoid field offsets due to flux trapped in the sample. In some samples the initial dip is at such a low field that it is not observed.

Figures 2a and 2b show the magnetization curves taken at a temperature of 60K for a crystal before and after a 200 hour, 460°C oxygen anneal, with calculated δ values of 0.25 and 0.14, respectively. These curves demonstrate that the magnetization features observed are controlled by the oxygen content as suggested earlier.[1,4] The resistivity and ac susceptibility of the unannealed crystal showed the broad transitions typically observed in oxygen-poor samples (Fig. 3a). After the anneal the transitions were 300mK wide (Fig. 3b). Details of these measurements are presented in reference 7.

Even though long oxygen anneals dramatically improve the crystals, full oxygenation is never achieved and a magnetization dip (at least at 60K) is always observed. There are clearly still inhomogeneities present. This observation brings into question whether large single crystals can ever be fully oxygenated, possibly because of the limitations imposed by the kinetics of the system at the low oxygenation temperatures. Another possible explanation is that these residual crystal inhomogeneities are due to cation disorder which would distort the c-axis versus δ relationship and would be unaffected by the oxygen anneals.

Figures 4a and 4b show data for three different crystals with different oxygen content, demonstrating the qualitative features of the magnetization that change with δ. Three striking features of these curves are:1) the shift in the position of the low field magnetization dip, H_{min}, 2) the shift in the high field magnetization maximum, H_{max}, and 3)the overall change in the magnitude of the magnetization. The second two features are due to the pinning behavior of vortices[1,4] and will not be discussed here.

In the critical state, the magnetization reflects the critical current density, J_c, which may be expressed in the standard Bean model form[11] $J_c \approx (M_+ - M_-)/2r$, where r is the radius of the region through which the screening currents flow. For a homogeneous material, r is identical to the radius of the sample, R, and the derived J_c will be independent of R. For an inhomogeneous material $r<R$ and the derived J_c depends on R. Thus, the homogeneity of a crystal can be tested by cleaving it and examining the magnetization as a function of R.

The size scaling data of reference 4 suggest that crystals are homogeneous for $H<H_{min}$ and inhomogeneous (or granular) for $H>H_{min}$. Welp et al.[5] performed a fracture experiment and claimed that the magnetization roughly scaled with size and was, therefore, homogeneous.

We conducted similar breaking studies on several crystals in order to explore their homogeneity. The results of a breaking experiment on a crystal with $\delta \sim 0.16$ and $H_{min} \sim 1T$ are shown in figure 5a. The data are presented in the standard Bean model form with $R=(3/2)w(1-(w/3l))$ for the crystal face of length, l and width, w.[11] We see that for this specimen J_c is approximately independent of R at low fields with deviations becoming evident in the range $H \approx 1\text{-}2T$. Thus the breakdown of scaling occurs at a field value close to H_{min}.

Figure 5b shows similar data for a crystal with $\delta \sim 0.21$ which shows neither the low field decrease nor size scaling at any field. The raw magnetization data for this crystal look similar to that of Welp et al.[5], where the magnetic moment of a crystal was measured before and after fracturing. They found that the samples' magnetic moment, m, approximately scaled with the mean fragment size and thus concluded that there was no evidence of granular behavior. This interpretation can be misleading since the magnetization does decrease with R, but not as predicted by the Bean model. This partial scaling of the magnetization implies that there is a distribution of current paths, some of which are smaller than the sample radius, rather than isolated current loops flowing around decoupled "grains". This result is consistent with the earlier work[2,3] and is predicted for a percolating system.[12]

There is a degree of uncertainty in the relationship between the onset of granularity and the position H_{min} since the dip is the result of the interplay between the magnitude of the intrinsic pinning and the intergranular coupling[4]. Therefore, as δ decreases, the coupling improves, the pinning (which is most likely at the defects) decreases, and the minimum becomes less well defined (Fig. 4). However, the size scaling results clearly show the onset of granular behavior at fields near H_{min}.

Figure 6a, summarizing the $H_{min}(\delta,T)$ results, resembles a phase diagram with H_{min} representing a phase boundary which determines whether or not a crystal is "granular" for a given δ and T. These curves reflect the $J_c(T)$ behavior for the microscopic oxygen-defect regions which define "grain boundaries." For temperatures near T_c, $H_{min}(T)$ is almost independent of temperature and increases with decreasing δ. As the temperature decreases, $H_{min}(T)$ increases rather sharply. This behavior is consistent with the relatively large intergranular J_c's expected for well oxygenated crystals and the increase in J_c (and subsequent loss of 'granularity') anticipated at low temperatures.

Discussion & Interpretation

One significant difference between high T_c superconductors (HTS) and classical, low temperature superconductors is the small coherence lengths of the HTS. Since the coherence length in the a-b plane, ξ_{ab}, of the "123" system is so small (~10-15Å) supercurrents

are easily perturbed by microscopic inhomogeneities[13,14]. Whereas isolated defect regions with dimensions of the order of ξ_{ab} should be ideal pinning centers, extended regions with a thickness of that size (or smaller) will impede the supercurrent flow when the current density exceeds the local $J_c(H,T)$.

Contamination from the alumina, gold, or MgO crucibles used in crystal growth undoubtedly contributed to the inhomogeneity of crystals in some of the earlier work. As stated above, the contamination due to the zirconia crucibles used in the synthesis of the crystals used in this study is below observable levels. We therefore assume that the observed magnetization behavior is due principally to oxygen defects.

The perturbing inhomogeneity boundaries can form at rather low oxygen defect densities. We can estimate the value of δ for which supercurrents become sensitive to defects by assuming a uniform defect density and currents that flow in independent layers. The last assumption is reasonable considering the anisotropy of the system. Since superconductivity is a reflection of the properties of a material averaged over a coherence volume, we also assume that the coherence length in the a-b plane is approximately independent of δ.

The average distance between defects in the a-b plane[4] is $\sim a/\sqrt{\delta}$. Using $a \sim 3.8$Å and $\xi_{ab} \sim 15$Å, we estimate that, for currents circulating in the a-b planes of a crystal, defects are separated by one coherence length when $\delta \sim 0.06$. Such a crystal should not exhibit granular effects since it is uniform. (Several groups[15-17] have reported conditions which produce samples with ordered

defects and exhibit depressed T_c's.) As the crystals deviate from uniformity, extended defect-free regions surrounded by higher-δ "boundaries" are formed.

The pervasive presence of the oxygen sensitive magnetization anomalies, along with the difficulty in preparing samples with ordered defects, leads us to conclude that a realistic analysis of samples synthesized with conventional oxygenation regimens (i.e. slow cools and/or long soaks) must include the effects of defect density fluctuations. A percolation model, in which oxygen defects randomly populate the chains, is the natural choice for describing how these defect fluctuations create oxygen poor "grain boundaries." Since the superconductive properties of "123" are a function of δ, these local fluctuations in the oxygen content (local being defined as a square of ξ_{ab}, or about four units cells, on each side) then modify the local properties of the sample creating regions with differing resistivities, critical current densities, transition temperatures and critical fields. The result will be a distribution of current paths as currents flow through regions of least resistance at a given temperature and field. Since regions of lower and higher T_c are then in intimate contact, there should be a contribution from proximity effects to the J_c and H_c of the boundaries.

Assuming a random distribution of oxygen defects, $p=1-\delta$ is the occupation probability of oxygen in a unit cell. There exists a critical oxygen deficiency, δ_c, above which there are no continuous current paths. The scaling theory of percolation clusters predicts[18] that for electrical conductivity, $\sigma \sim (p-p_c)^{\mu}$ or $(\delta_c-\delta)^{\mu}$ near δ_c. The

critical exponent, μ, has been found to be 1.7 in three dimensions and 1.2 in two[18].

Adopting this percolation framework Kubo et al.[19] have employed Monte Carlo simulations for a two dimensional square lattice and found $\delta_c \sim 0.26$. For δ greater than 0.26 oxygen rich, superconducting "grains" are separated by oxygen poor, insulating boundaries so that there is no superconducting path through a sample. For δ less than 0.26, a complete current path spans the sample and resistance measurements show metallic behavior with a superconducting transition.

In figure 6b we plot H_{min} as a function of δ for three different temperatures. A remarkable feature of these curves is that $H_{min}(T)$ extrapolates to zero near $\delta \sim 0.20$. Since H_{min} signals the onset of granularity, a sample with $H_{min}=0$ implies that the crystal has so many oxygen defects that it never exhibits single-grain behavior. The convergence of the three temperature curves at a δ near the 0.26 predicted by Kubo et al.[19] suggests that the two-dimensional percolation picture is appropriate. The temperature independence of that critical point indicates that the coupling of the isolated grains is virtually temperature independent at these temperatures.

Encouraged by these observations, we present the following argument which makes the connection between H_{min} and δ. Just as a dc critical current measurement of an inhomogeneous material reflects a distribution of weak link regions, so should H_{min} reflect this granularity in a magnetization measurement. As percolation theory predicts and experiments have confirmed[12,20,21]

$J_c \sim (p-p_c)^{(d-1)\nu}$ or $(\delta_c-\delta)^{(d-1)\nu}$ with ν=1.35 and 0.9 for two and three dimensions respectively, exponents similar to those for conductivity. H_{min}, being sensitive to these weak links, should scale in a similar manner and provide a sensitive probe of the onset of percolation. We can then correlate the shape of the boundary in the H_{min}-δ phase diagram with the scaling law for critical current density in the inhomogeneous system.

As Kubo and Igarashi[19] pointed out, it is difficult to incorporate effects of local ordering into such a model. Fortunately, it is not necessary to know the details of the complex relationships between the superconducting parameters and δ to understand the general behavior of the magnetization dip, only that the currents will seek the paths of least resistance and that these paths are uncorrelated[12]. Since J_c is a function of temperature and oxygen content, a scaling relation of the form $H_{min} \sim C(T)|\delta_c-\delta|^m$ should describe the shape of the boundary curve. A least squares fit of the rather scattered 60K data to that power law (figure 7) gives δ_c=0.22±0.03 and m=1.4±0.5. The results are consistent with both the Kubo and Igarashi[19] value for δ_c and the above power law for two or three dimensional percolation.

It is likely that the subgranularity will be manifested in other electrical measurements. Resistivity measurements in the presence of an applied magnetic field show a broadening of the transition particularly for H⊥J. This broadening has been qualitatively fit to a Bardeen-Stephen flux-flow model.[22] Measurements of the angular dependence of the resistivity in the transition also fit well within a flux-flow model.[23] However, an angular-independent background

resistance is not accounted for in these simple flux-motion models, most likely because such models neglect the effects of granularity. These models assume a homogeneous superconductor in which the dissipation is due to the viscous flow of Lorentz-force-driven vortices. However, with the granularity/weak-link nature of these materials, one would expect broadening of the transition even in the force-free configuration (H||J) due to the percolative nature of the system.

CONCLUSIONS

We have used magnetization as a sensitive tool to validate the "quality" of $YBa_2Cu_3O_{7-\delta}$ crystals. The observed dip in the magnetization signals the onset of granularity due to locally oxygen depleted regions and correlates with average oxygen content via the c-lattice parameter. We construct an H_{min}-temperature pseudo phase diagram with boundaries that separate the phase space into single-grain and multigrain regimes for each δ. By plotting the same data in an H_{min}-δ diagram, the percolative nature of the problem becomes apparent. The data at 60K follow an $H_{min} \sim C(\delta_c-\delta)^{\mu}$ scaling law with δ_c close to a predicted value of 0.26 and μ of 1.4 which is consistent with the scaling law for critical currents in two or three dimensions.

The authors wish to acknowledge helpful discussions with Mark Reeves and Guy Deutscher and the support of the Office of Naval Research (ONR),

DARPA. J.L.C. and M.M.M. acknowledge support from The Office of Naval Technology (ONT) and National Research Council (NRC), respectively.

REFERENCES

1. H. Kupfer, I. Apfelstedt, R. Flukiger, C. Keller, R. Meier-Hirmer, B. Runtsch, A. Turowski, U. Wiech, and T. Wolf, Cryogenics **29**, 268(1989)

2. A. Sulpice, P. Lejay, R. Tournier, and J. Chaussy, Europhys. Lett. **7**, 365(1988)

3. Y. Yeshurun, M. W. McElfresh, A. P. Malozemoff, J. Hagerhorst-Trewhella, J. Mannhart, F. Holtzberg, and G. V. Chandrashekhar, Phys. Rev. B **42**, 6322(1990)

4. M. Daeumling, J.M. Seuntjens, and D.C. Larbalestier, Nature **346**, 332(1990)

5. U. Welp, W.K. Kwok, G.W. Crabtree, K.G. Vandervoort, and J.Z. Liu, Appl. Phys. Lett. **57**, 84(1990)

6. M.E. Parks, A. Navrotsky, K. Mocala, E. Takayama-Muromachi, A. Jacobson, and P.K. Davies, J. Solid St. Chem. **79**, 53(1989)

7. T.A. Vanderah, C.K. Lowe-Ma, D.E. Bliss, M.W. Decker, M.S. Osofsky, E.F. Skelton, and M.M. Miller, submitted to J. Crystal Growth

8. W. Sadowski and H.J. Scheel, J. Less-Common Metals **150**, 219(1989)

9. J.S. Swinnea and H. Steinfink, J. Mater. Res. **2**(4), 428 (1987)

10. E.H. Appelman, L.R. Morss, A.M. Kini, U. Geiser, A. Umezawa, G.W. Crabtree, and K.D. Carlson, Inorg. Chem. **26**(20), 3237 (1987)

11. E.M. Gyorgy, R.B. Van Dover, K.A. Jackson, L.F. Schneemeyer, and J. V. Waszczak, Appl. Phys. Lett **55**, 283(1989)

12. G. Deutscher, "Short Coherence Length and Granular Effects in Conventional and High T_c Superconductors," in **Superconductivity,** eds. J. G. Bednorz and K. A. Muller, pp.174-200, Springer-Verlag, Berlin Heidelberg, 1990

13. Tinkham and C. J. Lobb, "Physical Properties of the New Superconductors," Solid State Physics, V.42, p91, Eds H. Ehrenreich and D. Turnbull, Academic Press, 1989

14. G. Deutscher, "Percolation and Superconductivity," Percolation, Localization, and Superconductivity, eds. A.M. Goldman and S.A. Wolf, Plenum, p95(1984)

15. R.J. Cava, B. Batlogg, C.H. Chen, E.A. Rietman, S.M. Zahurak, and D.J. Werder, Nature **329**, 423 (1987); Phys. Rev. B **36**, 5719 (1987)

16. J.D. Jorgensen, B.W. Veal, A.P. Paulikas, L.J. Nowicki, G.W. Crabtree, H. Claus, and W.K. Kwok, Phys. Rev. B **41**, 1863 (1990)

17. R. Beyers, B.T. Ahn, G. Gorman, V.Y. Lee, S.S.P. Parken, M.L. Ramirez, K.P. Roche, J.E. Vazquez, T.M. Gur, and R.A. Huggins, Nature **340**, 619 (1989)

18. D. Stauffer, Phys. Rep. **54**, 1(1979)

19. Y. Kubo and H. Igarashi, Phys. Rev.**B 39**, 725(1989)

20. M. Tinkham, "Introduction to Inhomogeneous Superconductors," Inhomogeneous Superconductors-1979, eds. D.U. Gubser, T.L.Francavilla, J.R. Leibowitz and S.A. Wolf, American Institute of Physics, p1(1980)

21. G. Deutscher, O. Entin-Wohlman, M. Rappaport, and Y. Shapira, "Critical Behavior of Percolating Superconductors," Percolation, Localization, and Superconductivity, eds. A.M. Goldman and S.A. Wolf, Plenum, p23(1984)

22. A.P. Malozemoff, T.K. Worthington, E. Zeldov, N.C. Yeh, M.W. McElfresh, and F. Holtzberg, from Strong Correlations and Superconductivity, ed. H. Fukuyama, S. Maekawa, and A.P. Malozemoff, Springer, Heidelberg, 1989.

23. W.K. Kwok, U. Welp, G.W. Crabtree, K.G. Vandervoort, R. Hulscher, and J.Z. Liu, Phys. Rev. Lett. 64, 966 (1990).

TABLE AND FIGURE CAPTIONS

Table 1. List of the last stage of the sample anneals and their resulting c-axis lattice parameters and corresponding oxygen content as determined in the text. Anneals were performed in oxygen unless otherwise stated.

Figure 1. Magnetization loop of crystal #3 with $\delta \cong 0.17$ at several temperatures showing the change of H_{min} with temperature. Figure (b) expands the low field region of (a) and the arrows indicate the positions of $H_{min}(T)$.

Figure 2. The 60K magnetization loop of crystal #14 before and after annealing demonstrating that H_{min} is controlled by oxygen content. Figure (b) expands the low field region of (a) and the arrows indicate the positions of $H_{min}(\delta)$.

Figure 3. Resistivity and ac susceptibility of the crystal in figure 2 before (a) and after (b) annealing.

Figure 4. Magnetization loops of crystals 3, 9, and 12 with δ=0,17, 0.06, and 0.21 respectively at 60K showing the dependence of H_{min} on oxygen content. Figure (b) expands the low field region of (a) and the arrows indicate the positions of $H_{min}(\delta)$.

Figure 5. Results of the breaking experiment on (a) crystal #5 with $\delta \sim 0.16$ and $H_{min} \sim 1T$ and (b) crystal #13 with $\delta \sim 0.21$ and $H_{min} \sim 0$ presented in the standard Bean model form, $J_c \approx (M_+ - M_-)/2R$, where $R=(3/2)w(1-(w/3l))$ is the radius of the crystal face of length l and width w.

Figure 6. (a)Summary of the $H_{min}(\delta,T)$ results which resembles a phase diagram with H_{min} representing a phase boundary which determines whether a crystal is "granular" or not for a given δ and T. (b) Plot of H_{min} as a function of δ revealing curves for each of three temperatures converging near $H_{min} \sim 0$ at $\delta \sim 0.20$. The lines are linear fits to the data.

Figure 7. The 60K data of figure 6b. The line is a least squares fit of the data to the function $H_{min}=C(T)|\delta_c-\delta|^m$.

Sample	Batch	Anneal	c (Å)	δ
1	A	565°C/14 days	11.696	0.20
2	A	565°C/21 days*	11.695	0.19
3	A	565°C/21 days*	11.691	0.17
4	A	565°C/21 days	11.693	0.18
5	B	440°C/7 days	11.689	0.16
6	A	565°C/28 days	11.691	0.17
7	C	475°C/8.3 days	11.687	0.15
8	C	565°C/96h	11.692	0.18
9	B	475°C/8.3 days	11.684	0.13
10	B	475°C/8.3 days	11.672	0.06
11	D	515°C/3 days	11.695	0.19
12	D	515°C/3 days	11.693	0.18
13	E	565°C/96h	11.698	0.21
14	F	540°C/6 days	11.695	0.19
15	E	unannealed	11.703	0.25
15A	E	460°C/15.5 days	11.685	0.14
16	G	505°C/8 days	11.683	0.12
17	H	475°C/8 days	11.686	0.14
18	D	450°C/8 days	11.682	0.12
19	E	450°C/16 days*	11.6858	0.15
20	I	420°C/10days	11.681	0.11

*+460°C/5 minutes/air for de-twinning

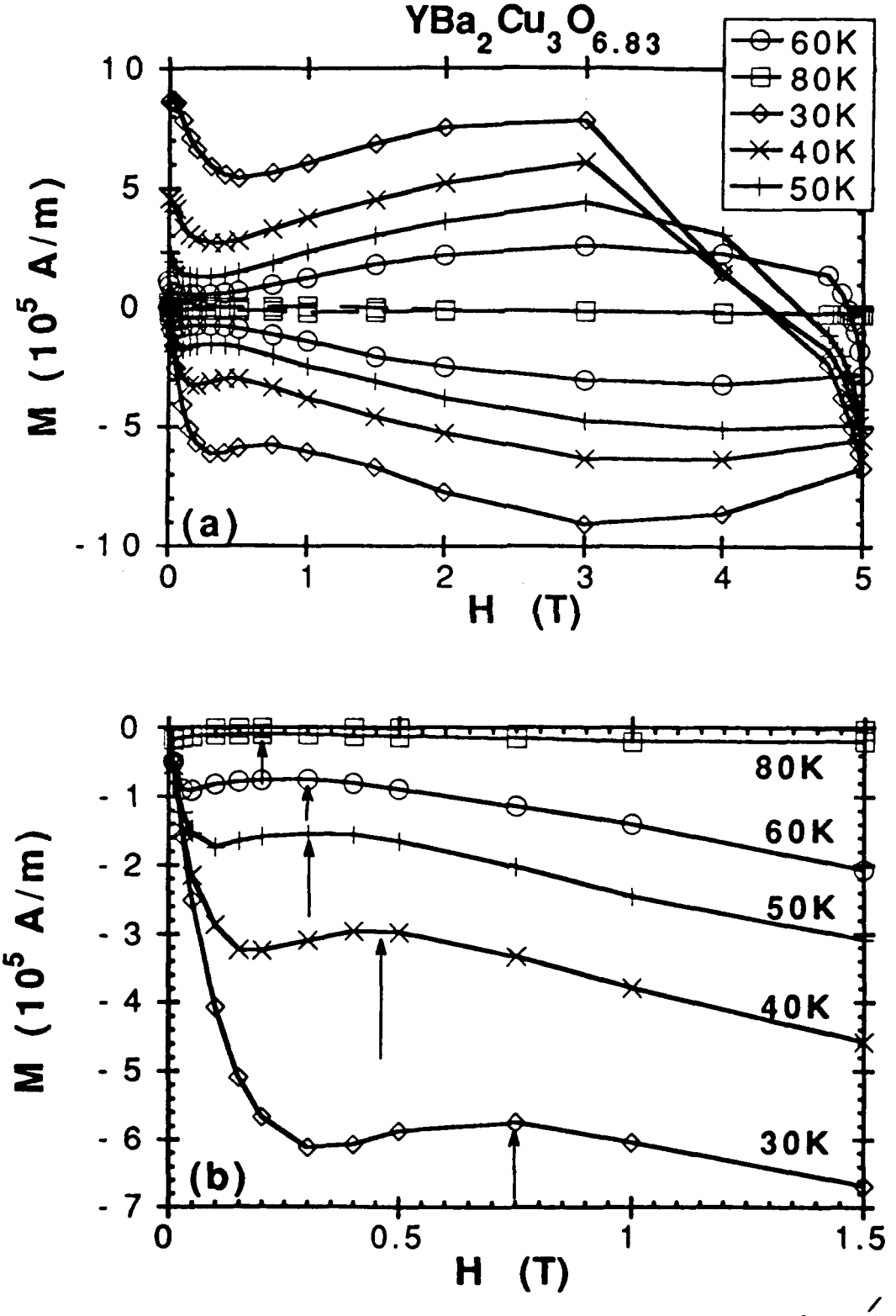
YBa2Cu3O6.83
60K
80K
30K
40K
50K
M (10^5 A/m)
H (T)
(a)
(b)
80K
60K
50K
40K
30K

Fig. 1

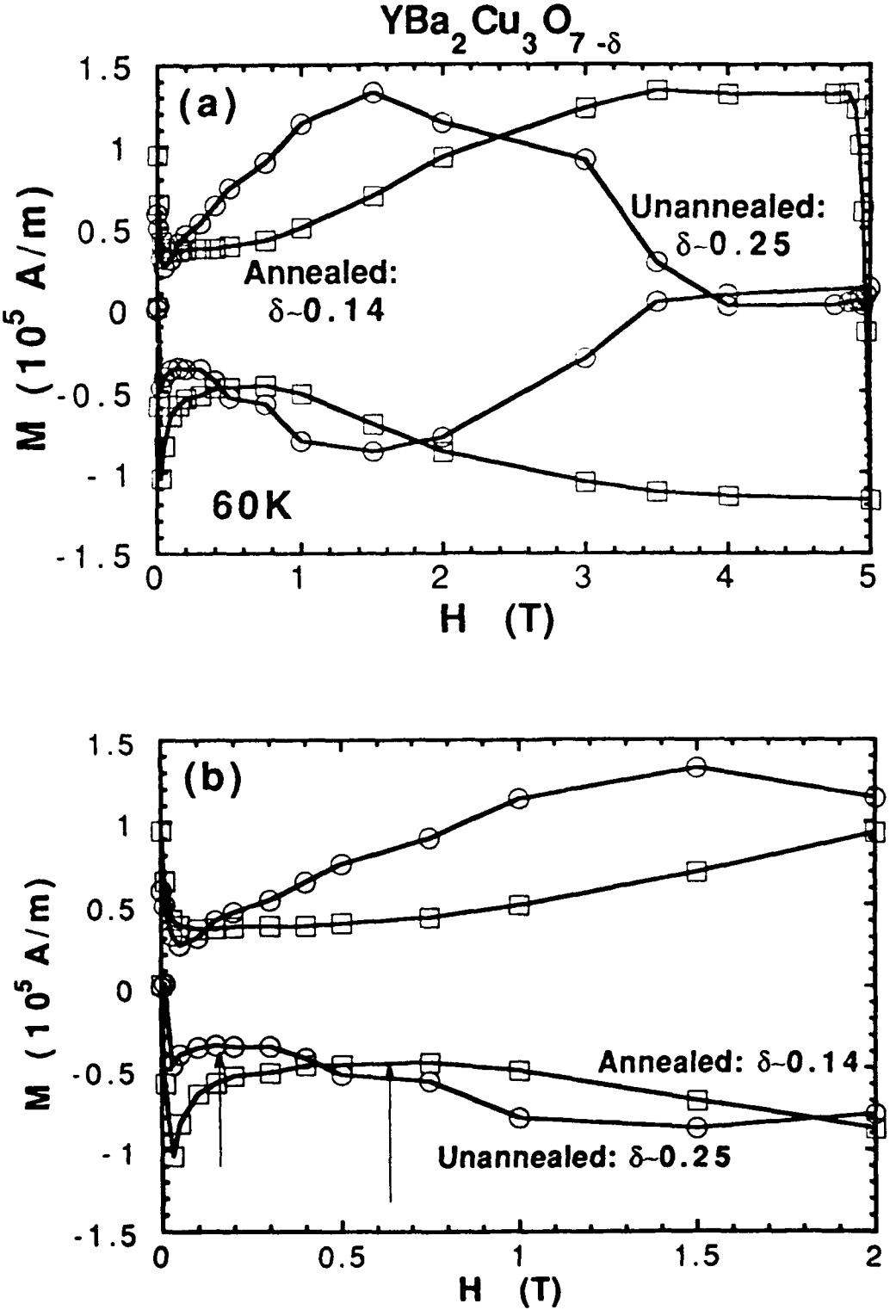
YBa2Cu3O7-δ
(a)
Annealed:
δ~0.14
Unannealed:
δ~0.25
60K
M (10^5 A/m)
H (T)
(b)
Annealed: δ~0.14
Unannealed: δ~0.25
M (10^5 A/m)
H (T)

Fig. 2

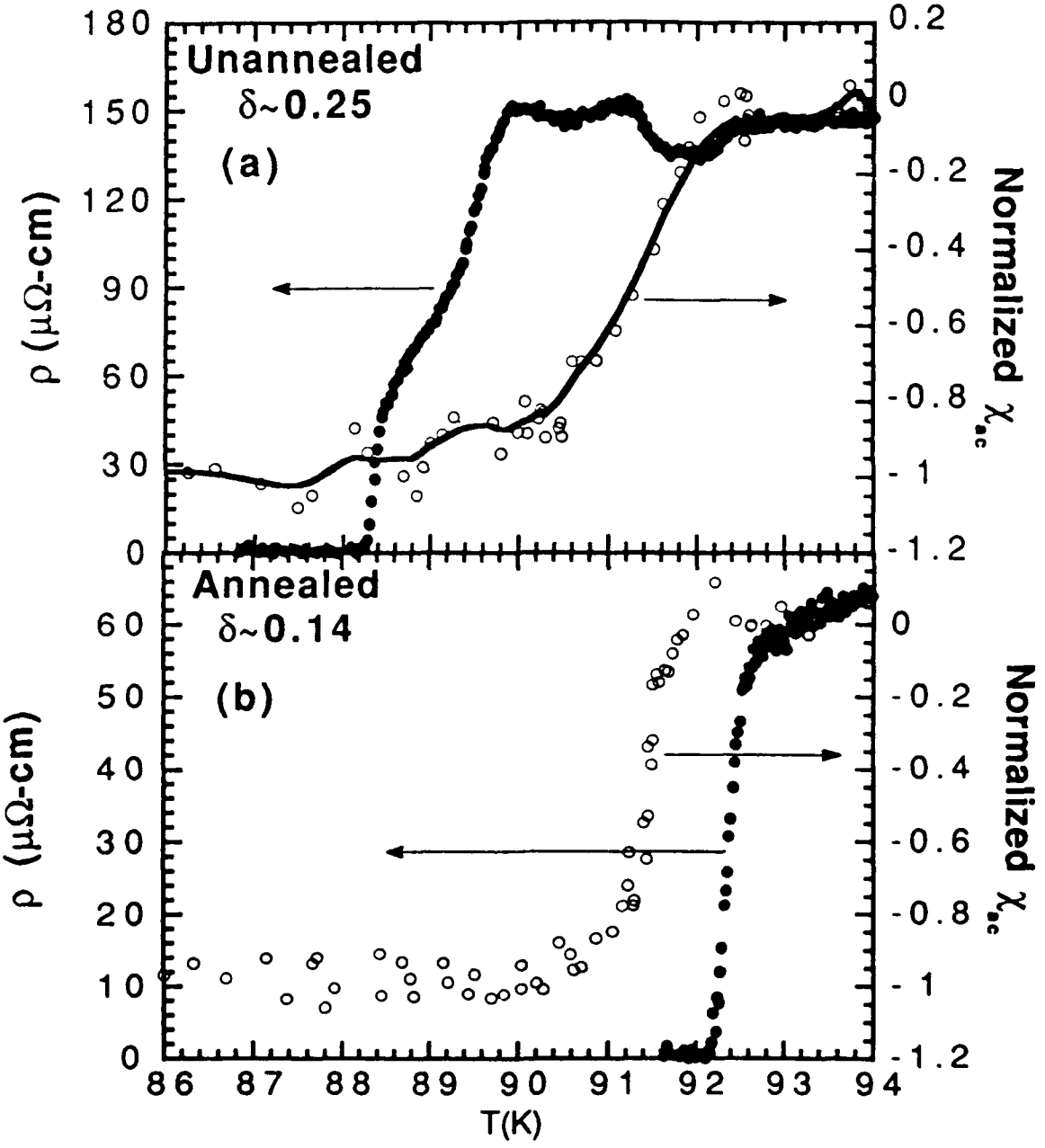
Unannealed
δ~0.25
(a)
Annealed
δ~0.14
(b)
ρ (μΩ-cm)
Normalized χ_{ac}
T(K)
180
150
120
90
60
30
0
50
40
20
10
0.2
-0.2
-0.4
-0.6
-0.8
-1
-1.2
86
87
88
89
90
91
92
93
94

Fig. 3

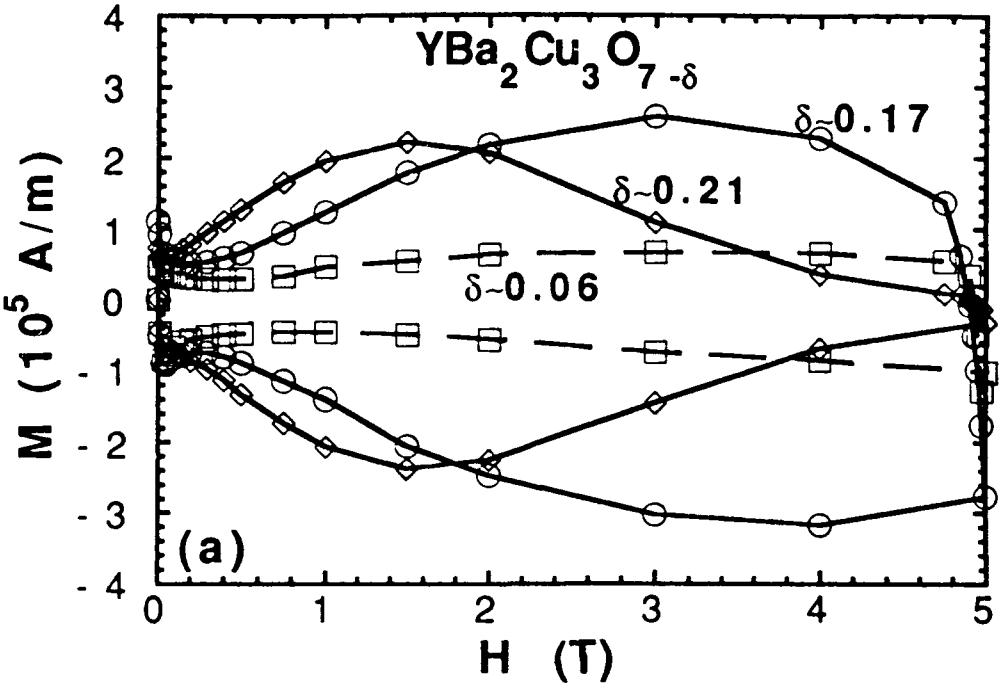
YBa2Cu3O7-δ
δ~0.17
δ~0.21
δ~0.06
(a)
M (10^5 A/m)
H (T)
4
3
2
1
0
- 1
- 2
- 3
- 4
0
1
2
3
4
5

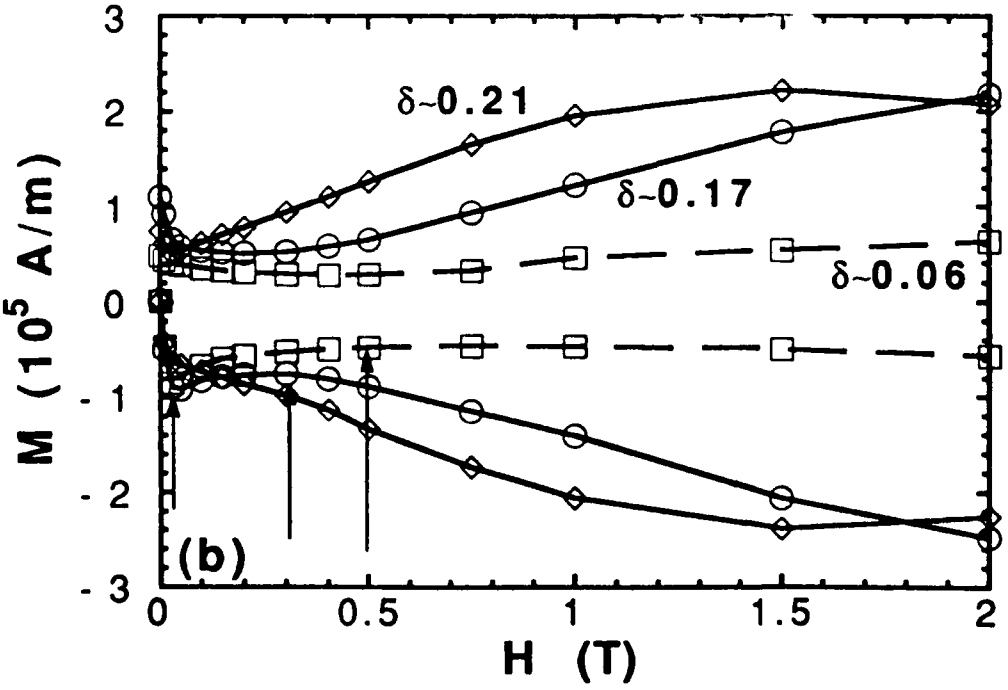
δ~0.21
δ~0.17
δ~0.06
(b)
M (10^5 A/m)
H (T)
3
2
1
0
- 1
- 2
- 3
0
0.5
1
1.5
2

Fig 4

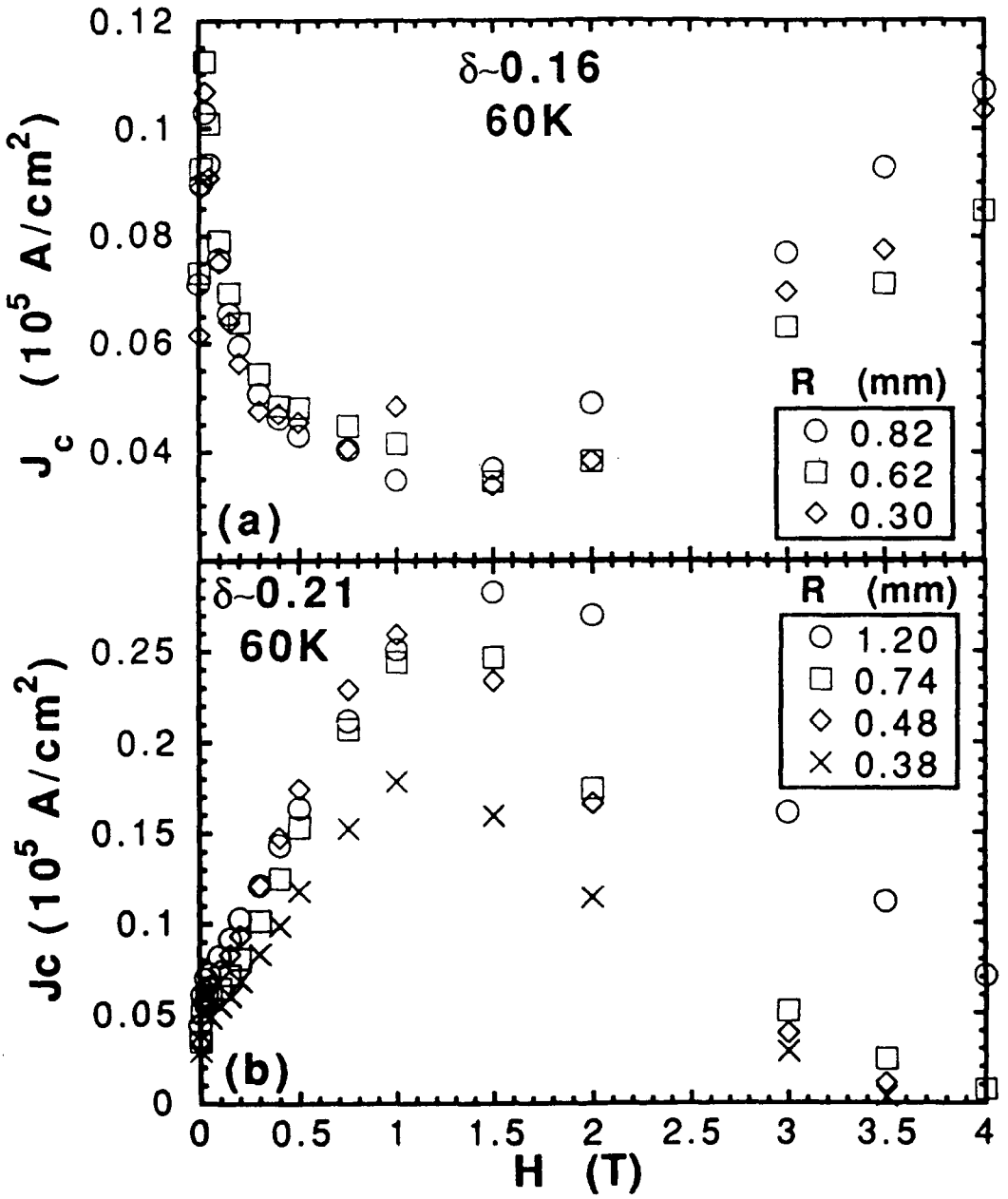
δ~0.16
60K
(a)
R (mm)
0.82
0.62
0.30
δ~0.21
60K
(b)
R (mm)
1.20
0.74
0.48
0.38
J_c (10^5 A/cm^2)
Jc (10^5 A/cm^2)
H (T)
0.12
0.1
0.08
0.06
0.04
0.25
0.2
0.15
0.1
0.05
0
0
0.5
1
1.5
2
2.5
3
3.5
4

Fig. 5

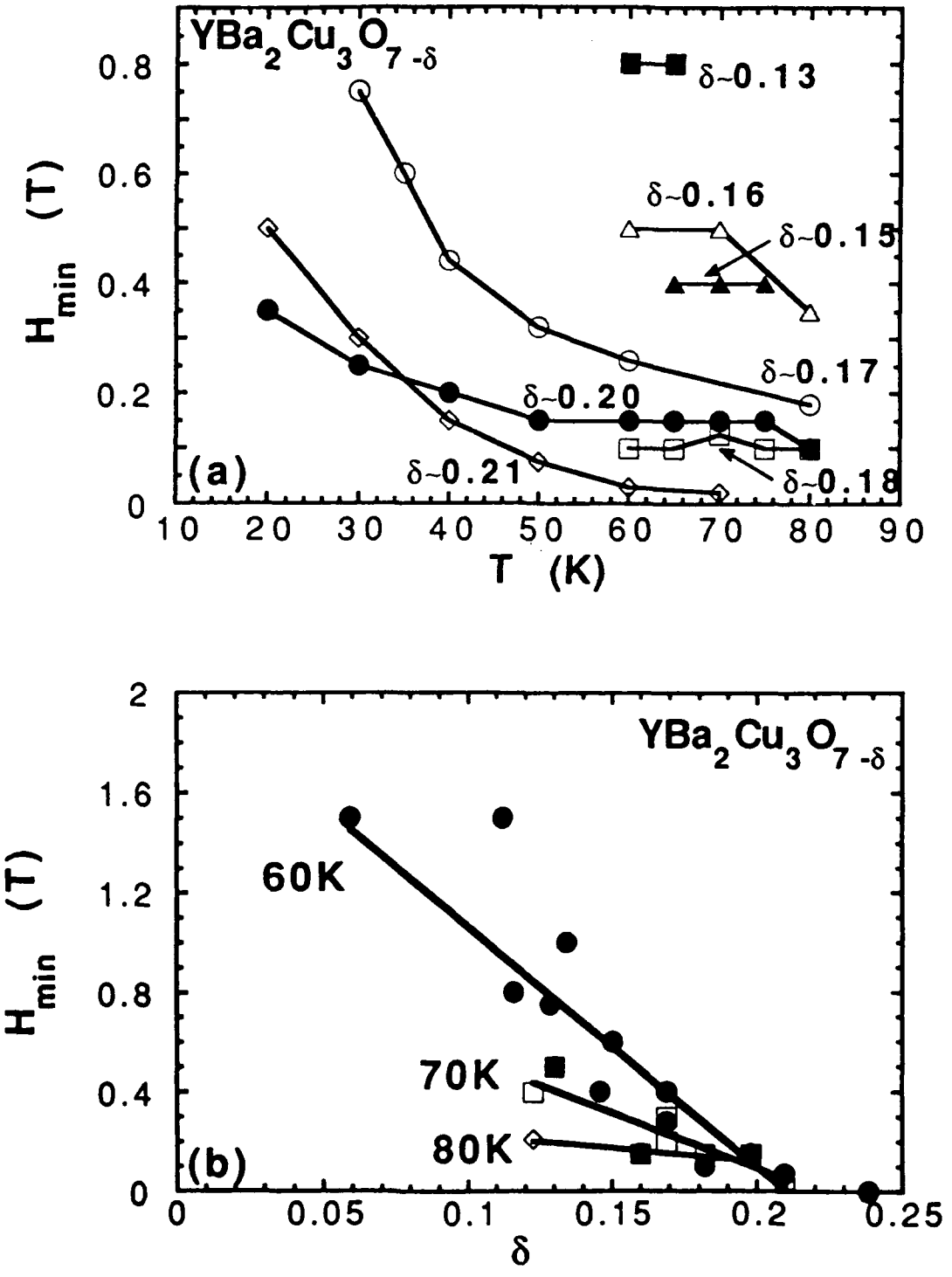
YBa2Cu3O7-δ
δ~0.13
δ~0.16
δ~0.15
δ~0.17
δ~0.20
δ~0.21
δ~0.18
(a)
Hmin (T)
T (K)
0
0.2
0.4
0.6
0.8
10
20
30
40
50
60
70
80
90
YBa2Cu3O7-δ
60K
70K
80K
(b)
Hmin (T)
δ
0
0.4
0.8
1.2
1.6
2
0.05
0.1
0.15
0.2
0.25

Fig. 6

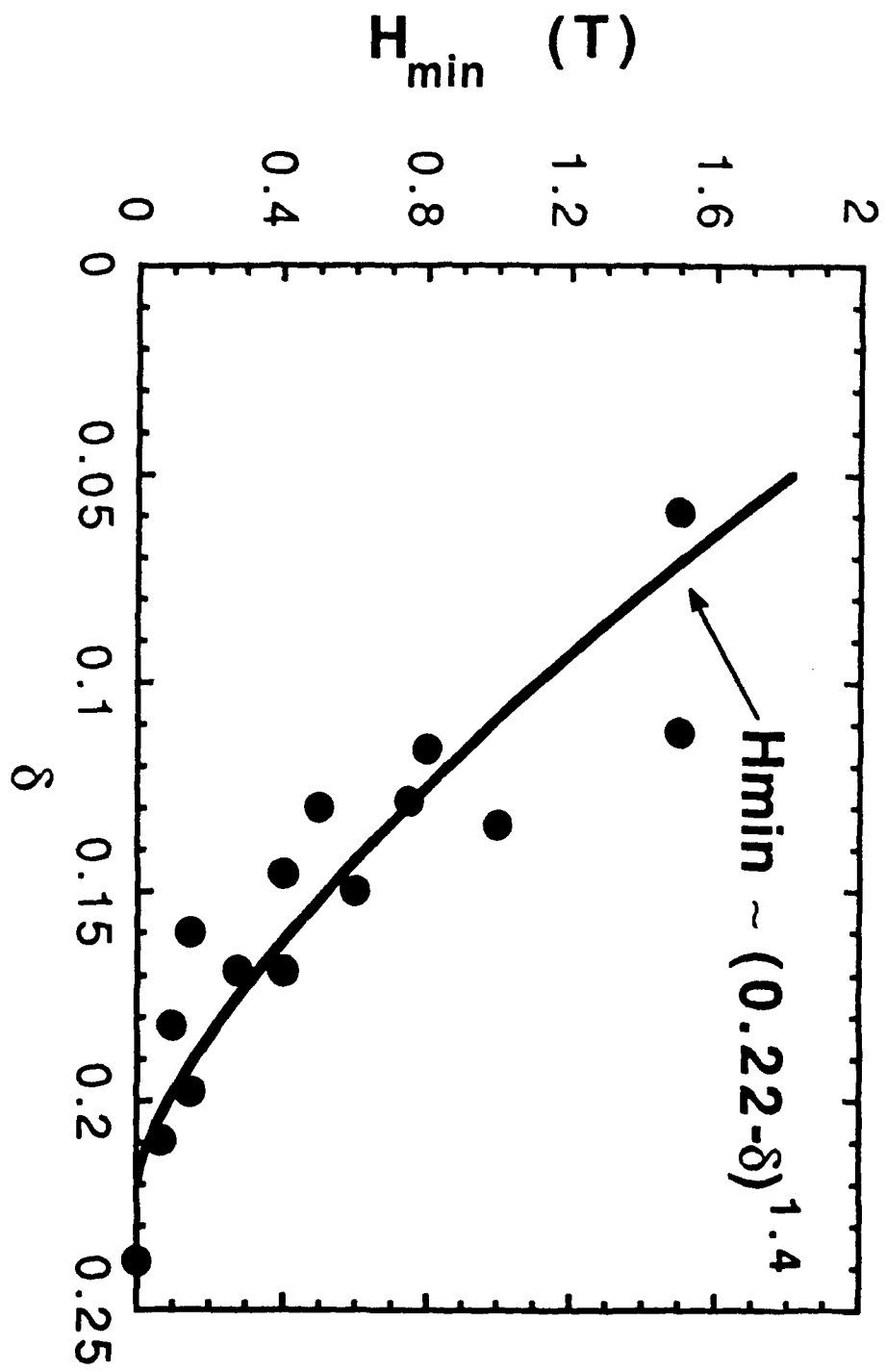

Fig. 7